Energy and Exergy Analysis of Modular Data Centers

Rehan Khalid, Aaron P. Wemhoff, and Yogendra Joshi, *Fellow, IEEE*

***Abstract*—The data center industry focuses on initiatives to reduce its enormous energy consumption and to minimize its adverse environmental impact. Modular data centers provide considerable operational flexibility in that they are mobile and are manufactured using standard containers. This paper develops steady-state energy and exergy destruction models for modular data centers with the open-source EnergyPlus software package. Three different cooling approaches are examined: direct expansion (DX) cooling, evaporative cooling (direct evaporative cooling, DEC, in this study), and free air cooling (air-side economization in this study). This paper shows that for hot and arid climates like those in the southwestern U.S., augmenting DX cooling with evaporative and free air cooling can result in energy savings of up to 38% and 36%, respectively. This paper also applies exergy analysis to suggest that the Energy Reuse Effectiveness of the data center increases with decreasing ambient (outdoor) temperature and increasing server inlet–outlet temperature difference. Furthermore, simulations indicate that the use of passive cooling techniques (e.g., DEC and free air cooling) decrease data center heating, ventilation, and air-conditioning energy consumption, except in extremely hot and humid climates.**

***Index Terms*—Cooling, data center, energy efficiency, EnergyPlus (EP), exergy analysis, free air cooling, power usage effectiveness (PUE).**

NOMENCLATURE

$c_{p,a}$	Specific heat capacity at constant pressure of air.
COP	Coefficient of performance.
CFD	Computational fluid dynamics.
CPU	Central processing unit.
CRAC	Computer room air conditioner.
CRAH	Computer room air handler.
CSV	Comma-separated values.
DEC	Direct evaporative cooling.
DX	Direct expansion.
EMS	Energy management system.
EP	EnergyPlus.
ERE	Energy reuse effectiveness.
HVAC	Heating, ventilation, and air-conditioning.
IDF	Input data file.
IT	Information technology.
$\dot{m}$	Mass flow rate of cooling air.
NREL	National Renewable Energy Laboratory.
PUE	Power usage effectiveness.
$\dot{Q}$	Power dissipation in the form of heat.
R_s	Resistance of Server.
SCOP	Sensible coefficient of performance.
T	Temperature.
W	Power dissipation in the form of work.
VAV	Variable air volume.

Symbols

$\dot{\Psi}_d$	Rate of exergy destruction.
ψ	Exergy.
g	Gravitational acceleration constant.
h	Enthalpy.
s	Entropy.
z	Elevation.

Subscripts

e	Exit.
fan	Cooling fan.
i/in	Inlet.
out	Outlet.
ref	Reference/ambient.
s	Server.

Manuscript received October 15, 2016; revised April 13, 2017; accepted May 4, 2017. Date of publication June 15, 2017; date of current version August 31, 2017. This work was supported in part by the National Science Foundation under Grant IIP-1134810, in part by the University Cooperative Research Center on Energy Efficient Electronic Systems at the Georgia Institute of Technology, and in part by Villanova University. Recommended for publication by Associate Editor M. Hodes upon evaluation of reviewers' comments. *(Corresponding author: Rehan Khalid.)*

R. Khalid and A. P. Wemhoff are with the Department of Mechanical Engineering, Villanova University, Villanova, PA 19085 USA (e-mail: rkhalid@villanova.edu; aaron.wemhoff@villanova.edu).

Y. Joshi is with the George W. Woodruff School of Mechanical Engineering, Georgia Institute of Technology, Atlanta, GA 30332 USA (e-mail: yogendra.joshi@gatech.edu).

Color versions of one or more of the figures in this paper are available online at http://ieeexplore.ieee.org.

Digital Object Identifier 10.1109/TCPMT.2017.2705055

I. INTRODUCTION

THIS paper discusses the impact of various cooling techniques on the performance of modular data centers. Regular brick-and-mortar-style data centers are common throughout the industry, but modular data centers are an emerging trend to enhance existing data center capacity or to deploy new capability in remote locations. Modular data centers have several advantages when compared to regular brick and mortar data centers. First, they are manufactured using standard shipping containers, retrofitted to suit the needs of the environment and the purpose for operation. Moreover, standard containers have the benefit of being pre-engineered, highly integrable,

relatively low-cost, and fast-moving, with deployment times of around a week. Finally, they are highly customizable to suit the needs of the data center operator.

In traditional air-cooled data centers, an external mechanical chiller delivers cold water inside to cool the hot air. However, modular data centers, especially the all-in-one type, discussed in this paper, cannot have components external to the system (e.g., electrical or mechanical system containers) since this approach sacrifices mobility. Moreover, modular data centers also do not rely on the raised-floor plenum for supplying cold air. However, the traditional hot and cold aisle arrangement of IT equipment, as well as augmenting the base cooling system with additional cost-effective cooling methodologies, are also employed in modular data centers.

Only a few selected studies specific to modular data centers are seen in the literature. Ham *et al.* [1] found that air-side economization for modular data centers could have significant savings (up to 67%) for specific climate regions. Further work by Ham *et al.* [2] showed the optimum supply air temperature for modular data centers to be in the 18 °C–23 °C range. They concluded that increasing the temperature any further increases the overall energy consumption since the reduction in chiller energy is offset by the increase in CRAH fan energy. Similar work on the use of fresh air for cooling container data centers by Endo *et al.* [3] showed that depending on the location, fresh air alone is not suitable to maintain the data center within ASHRAE's allowable range for data centers [4]. Their work suggests that supplementing fresh air with evaporative cooling and waste heat recovery from the data center can be used to effectively cool the facility even when the characteristics of fresh air were outside the ASHRAE allowable range. Similarly, Zhang *et al.* [5] reviewed the work done on free air cooling for data centers in general using air-side, water-side, and heat pipe free cooling. They concluded that heat pipe free cooling systems show the greatest energy efficiency and cooling capacity out of these three strategies because of their ability to transfer heat through small temperature differences without requiring external energy or moving parts, thus making them virtually maintenance-free. Qouneh *et al.* [6] compared the performance and efficiency of container data centers to that of raised-floor data centers. Their study concluded that containers achieve 80% and 42% savings in cooling and facility power, respectively, of that of a raised-floor data center, and that raised-floor data centers can approach the efficiency of a container at low utilizations, while using a single cooling optimization. Depoorter *et al.* [7] studied the effect of location on data center efficiency and its use as a renewable energy supply measurement tool. They examined five locations across Western Europe with climatic conditions ranging from Mediterranean-like in Barcelona, Spain, to arctic in Stockholm, Sweden. Their study suggested that the PUE rises in the summer months due to less availability of outside air with suitable conditions. Moreover, they noted that maximum energy consumption is tied with data center demand and occurs around mid-day. Thus, they suggested a smart IT management system to shift the load from peak hours to times in which electricity costs are cheaper to save energy and cut down on utility cost.

Studies on data center energy consumption, IT reliability and resiliency, and operating expenditure (OPEX) yield some interesting results. In a white paper by IBM [8], ASHRAE recommends operating data center IT equipment within their recommended envelope, for enhanced long-term reliability, and lower maintenance and replacement costs. However, for short-term use, such as in the event of a cooling system failure or malfunction, ASHRAE defines extended ranges or classes in which to operate IT equipment (classes A1, A2, and A3). However, operating long term in these classes can lead to reduced IT equipment reliability, lower data center resiliency and enhanced corrosion or electrostatic discharge of the equipment, depending on whether the IT equipment inlet relative humidity is higher or lower than the recommended range. In short, the choice of operation changes from facility to facility, and for different types of equipment, but operating out of the recommended range for longer periods of time is bound to increase OPEX. However, doing so in short bursts using techniques such as air-side or water-side economization can result in significant energy savings.

In a similar but more specific case, Alissa *et al.* [9] discuss the effect of cooling system failure on IT equipment, and the resulting uptime achieved using two different platforms: one through external sensors deployed outside IT equipment inlet grill, and the other using built-in sensors. They report higher uptimes using the external sensors, compared to the internal ones. They also report aisle containment to be less resilient than an open aisle configuration due to the formation of external impedances. They report $ 0.350M annual savings when the air inlet temperature setpoint is increased, and static pressure decreased, but this comes at the cost of 50% reduction in uptime in the event of a cooling failure. Clearly, these last two studies suggest a tradeoff between energy savings using passive techniques, and a reduction in resiliency of IT equipment in the event of a power failure and in case of operating long-term outside ASHRAE's recommended range.

The previous studies provide some insight into strategies to conserve energy in modular data centers, but the use of second-law thermodynamic analysis to compare different cooling solutions remains unexplored. This paper applies second-law thermodynamic analysis to compare how different cooling schemes affect the overall exergy destruction of the modular data center cooling system. The use of exergy destruction provides a means for incorporating the impact of mechanical and thermal work on the overall energy efficiency of the system, and how climate can affect the PUE. This approach is applied for modular data centers in selected climate regions in the U.S.

II. Methodology

A. Data Center Selection

This paper considers Huawei's 1000 A modular data center [10]. Fig. 1 shows the anatomy of this data center. Its construction and HVAC specifications are provided in Table I.

B. Modeling Tool Selection

Traditional data center modeling techniques include CFD, CFD-like numerical modeling, and thermodynamic modeling.

TABLE I
HUAWEI IDS 1000A SPECIFICATIONS

	Feature	IDS1000-A40
Size	External Dimensions (L*W*H)	12196*2438*2896(mm)
	Typical Power Capacity (rated)	60kW
	Typical Rack Capacity	8 IT Racks
Power	Power Density per Rack	5kW per rack (actual)
Cooling	Technology	DX type air-conditioner units
	Containment	Hot and Cold aisle isolation
	Cooling Capacity	12.5kW per unit
	Humidity	Optional humidifier
Design	Design target PUE	+ 1.6 at full load
Operation Parameters	Cold Aisle temperature	18-27°C within sensor tolerance
	Humidity Range	20% to 80% RH
Construction	Base Construction	40" standard ISO shipping container
	Insulation	Polyurethane: top-75mm, side-40mm

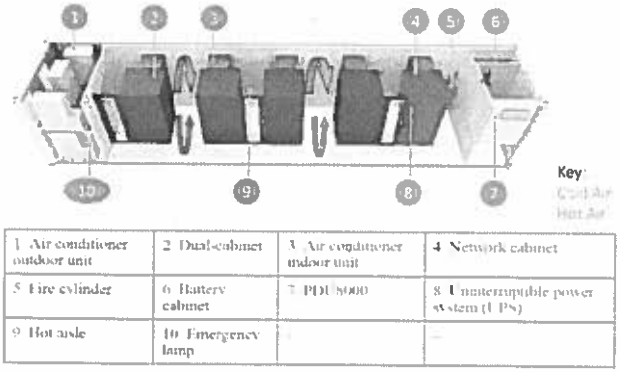

1 Air conditioner outdoor unit	2 Dual-cabinet	3 Air conditioner indoor unit	4 Network cabinet
5 Fire cylinder	6 Battery cabinet	7 PDU8000	8 Uninterruptible power system (UPS)
9 Hot aisle	10 Emergency lamp		

Fig. 1. Container data center layout description.

In CFD, a model of the entire dc airspace can be created and solved using the Navier–Stokes equations and then verified using experimental measurements and/or data to fit and improve the model. A key advantage of experimentally guided CFD is that once a model for a facility is created and validated, then various parameters can be varied to study the resultant effects to obtain optimum positioning and parameter values [11]. Similarly, CFD-like numerical modeling involves the use of turbulence models to numerically solve the Navier–Stokes and energy equations to predict the 3-D temperature distribution within a data center airspace [12]. Moreover, data center cooling and performance can be analyzed using thermodynamic models for power consumption and efficiency of various data center components [13].

The novelty of this paper lies in using EP as a data center modeling tool. EP was chosen because it is an open-source, and hence free, tool for building physics modeling that does not require implementing detailed CFD models. Currently, the tool does not explicitly support the modeling of data centers, and hence is being explored here as an alternative option for the thermal modeling of data centers.

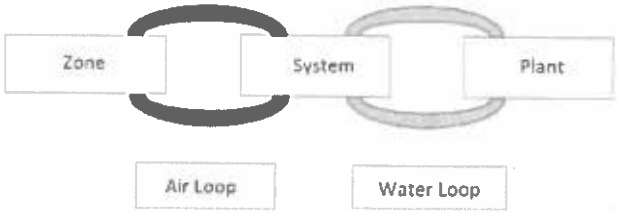

Fig. 2. Simultaneous solution scheme—EP.

Fig. 3. Selected locations across the U.S.

In EP, the entire data center can be represented as a series of functional elements connected by fluid loops, as shown in Fig. 2. The loops are divided into supply and demand sides, and the solution scheme generally relies on successive substitution iteration to reconcile supply and demand using the Gauss–Seidel scheme. The basis for the zone and air system integration is to formulate energy and moisture balances for the zone air, and solve the resulting ordinary differential equations using a predictor-corrector approach. Further details can be found in [14].

The geometry of the data center is modeled using Google's SketchUp, another freeware software that provides a graphical user interface [15].

C. Location and Climate

Fig. 3 shows the selected locations across the U.S., Chicago, IL, and Golden, CO, were selected as the prime locations for data center activity, with Tampa, FL, and Phoenix, AZ, chosen to simulate harsh environments and add detail to the comparison. The climate ranges from moist and cold in Chicago, to hot and dry in Phoenix. In general, the eastern half of the U.S. is in a moist climate zone, while the western half is in a dry climate zone, except for the Pacific coast, which is in a marine climate. Fig. 4 compares the outdoor dry-bulb temperature for each of the four chosen locations [16].

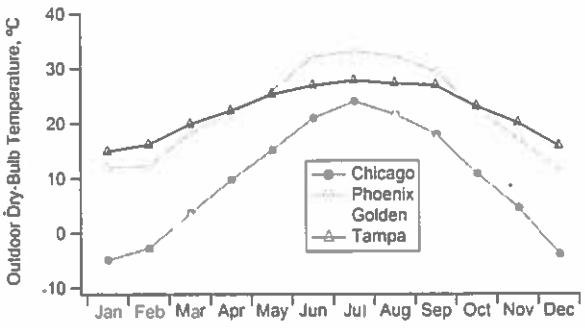

Fig. 4. Variation of outdoor dry-bulb temperature with location.

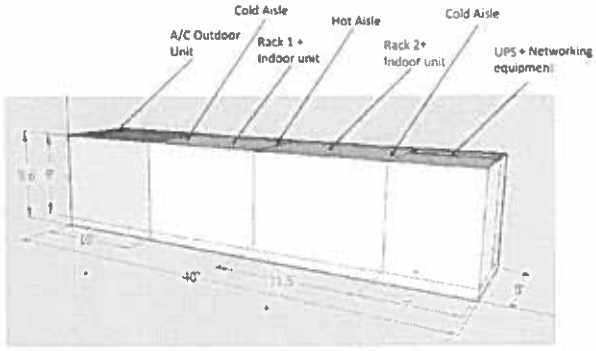

Fig. 5. Geometry created using SketchUp.

TABLE II
SOURCES OF HEAT GAIN WITHIN THE DATA CENTER

Source	Number of Units	Design Power (W)
Servers	100 (Dell R210)	500
Lights	--	300 (total)

III. MODEL DEVELOPMENT

A. Creating the Geometry

The geometry of the given size and construction was created using SketchUp. Two racks were modeled, thus creating one hot aisle, in the middle of the two racks, and two cold aisles. Two thermal zones were defined within SketchUp. Each cold aisle was one thermal zone, named cold zone, and the hot aisle was a second thermal zone, named hot zone. Two thermostats were similarly defined, one for the hot zone and the other for the cold zone. The geometry created using SketchUp is shown in Fig. 5.

B. Internal Gains

Lights and IT equipment were specified as sources of electric load. Table II lists the sources of heat gain along with their other characteristics.

The design CPU power can be modified using a built-in curve that calculates the actual CPU power (z) based on CPU loading (x) and inlet air temperature (y). A typical CPU power

TABLE III
CPU POWER MODIFIER CURVE

Coefficient	Default EP Value
C_1	-1
C_2	1.0
C_3	0.6
C_4	0.06667
C_5	0
C_6	0

Fig. 6. DX cooling system schematic.

modifier curve is a biquadratic function of the CPU loading schedule value (x) and the server inlet air temperature (y). The general form of a biquadratic curve is

$$z(x, y) = C_1 + C_2x + C_3x^2 + C_4y + C_5y^2 + C_6xy.$$

The loading curve coefficients are shown in Table III.

It should be noted that the biquadratic nature of this curve and the coefficient values shown in Table III are default to EP and have been used as such, unless otherwise noted. They are essential for enabling EP to calculate the power of IT equipment in a zone. This approach allows the user to modify this power to accurately simulate different types of equipment behavior.

C. Cooling System—DX Cooling

A DX cooling system contains a vapor compression refrigeration cycle with either an air-cooled or liquid-cooled condenser. As shown in Fig. 1, the evaporator is contained within the conditioned space, while the condenser is mounted on the outside walls of the container (not shown in Fig. 1) and cooled by the ambient air.

The HVAC schematic of a DX cooling system as detailed in EP is shown in Fig. 6. The specifications of the cooling system are provided in Table IV. The supply fan and DX cooling coil rated power and flow rate were autosized. This approach enables the software to calculate their value based on the cooling/heating setpoints and to design supply air temperature in order to meet the zone cooling load. The effects of filtration on fan power are assumed to be minor and are not included. Note that the presence of heating coils in Fig. 6 is merely a part of the EP DX component package, and heating is not used in this paper. In addition, EP accounts for site elevation on the air density for the EP energy calculations.

TABLE IV
DX COOLING SYSTEM SPECIFICATIONS

Object	Specification
System type	DX type A/C with electric heating
Thermostat type	Dual-zone thermostat
Heating Setpoint	15°C
Cooling Setpoint	29.3°C
Design Supply Air Temp.	14°C
Supply Fan	Variable speed fan
Air distribution unit	Single-duct VAV with no reheat
Cooling coil COP	4.6

If the air temperature at the coil's inlet is greater than both the supply equipment outlet node setpoint temperature (Node 2) and the cooling setpoint, then the cooling coil works to meet the setpoint at its exit, i.e., Node 1. In the opposite case, the cooling coil will remain OFF and the heating coil would work to meet the zone heating setpoint.

ASHRAE's environmental class A3 was specified as the guideline for incoming air to the servers for comparison of the HVAC system performance. The conditions for class A3 are 5 °C–35 °C inlet temperature and 8%–80% relative humidity. This class is chosen for reference purpose since it offers the most moderate conditions for data center cooling and is recommended for a wide variety of IT equipment. Higher classes such as A1 and A2 offer stringent conditions that lead to longer running of the cooling equipment and hence higher electricity consumption. Furthermore, they are recommended for a limited set of sophisticated equipment. As per ASHRAE class A3 conditions, the inlet temperature and relative humidity for this cooling system were met 100% of the time.

IV. PUE AND EXERGY CALCULATIONS

The EMS within EP allows the user to modify built-in functions such as schedules or setpoints for thermostats or to actuate various pieces of hardware. It also allows the user to declare EP variables as sensors and store their values to be used later. Hence, using these values, the PUE of the data center, SCOP of the cooling coil, and exergy destruction within the zone total airspace were calculated using EMS programs and reported at each time-step. The PUE is calculated as

$$\text{PUE} = \frac{\dot{Q}_{\text{total}}}{\dot{Q}_{\text{IT}}} \tag{1}$$

where $\dot{Q}_{\text{total}}$ and $\dot{Q}_{\text{IT}}$ are the total building load and IT load, respectively. The SCOP is calculated as

$$\text{SCOP} = \frac{\dot{Q}_{\text{DX,sens}} - \dot{Q}_{\text{fan}}}{\dot{W}_{\text{DX}} + \dot{W}_{\text{fan}}} \tag{2}$$

where $\dot{Q}_{\text{DX,sens}}$ is the sensible heat of the DX coil, $\dot{Q}_{\text{fan}}$ is the sensible heat input by the supply fan, $\dot{W}_{\text{DX}}$ is the power input to the DX coil, and $\dot{W}_{\text{fan}}$ is the power input to the supply fan. The effective server surface temperature, T_s, is calculated using a thermal resistance model as

$$T_s = T_{\text{in}} + \frac{T_{\text{out}} - T_{\text{in}}}{1 - \exp(-(R_s \dot{m}_s c_{p,a})^{-1})} \tag{3}$$

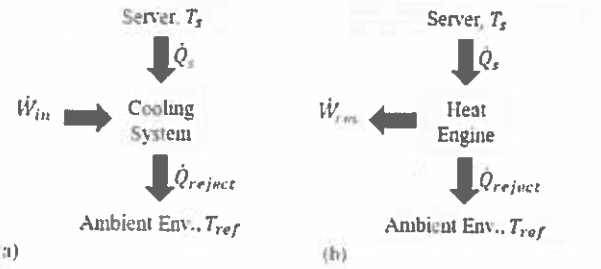

Fig. 7. (a) Simplified schematic of energy flows in a data center cooling system. (b) Application of data center heat to run a Carnot heat engine to produce reversible work.

where T_{in} and T_{out} are the air inlet and outlet temperatures, respectively; R_s is the server thermal resistance, $\dot{m}_s$ is the mass flow rate of air through the server, and $c_{p,a}$ is the specific heat capacity of air at constant pressure. The thermal exergy destruction in the servers is dominant in air-cooled data centers [17] and is calculated as [18]

$$\dot{\Psi}_{d,s} = n_s \left(\dot{m}_s c_{p,a} \left(T_{\text{in}} - T_{\text{out}} - T_{\text{ref}} \ln \left(\frac{T_{\text{in}}}{T_{\text{out}}} \right) \right) + \left(1 - \frac{T_{\text{ref}}}{T_s} \right) \dot{Q}_s \right) \tag{4}$$

where n_s is the number of servers, T_{ref} is the local ambient temperature, and $\dot{Q}_s$ is the heat output by the server. The final term in (4) refers to the rate of reversible work that accompanies heat flow.

A. Relationship Between ERE and Reference Temperature

The connection of exergy destruction and its impact on the ERE for different climate regions are straightforward using a general thermodynamic approach. Consider the basic system in Fig. 7(a). Heat ($\dot{Q}_{s,\text{tot}}$) is supplied from all servers at server temperature T_s. Mechanical work is added into a cooling system to reject the heat ($\dot{Q}_{\text{reject}}$) to the surroundings at T_{ref}. Following the standard thermodynamic analysis for a Carnot heat engine [19], as shown in Fig. 7(b), the rate of reversible work produced from the heat engine is $\dot{W}_{\text{rev}} = \dot{Q}_{s,\text{tot}} - \dot{Q}_{\text{reject}}$. Since $(\dot{Q}_{s,\text{tot}}/\dot{Q}_{\text{reject}}) = (T_s/T_{\text{ref}})$ in a reversible engine, then $\dot{W}_{\text{rev}} = \dot{Q}_{s,\text{tot}}(1 - (T_{\text{ref}}/T_s))$. Since the net mechanical work provided into the system for data center cooling systems is $\dot{W}_{in,\text{net}} = \dot{W}_{\text{in}} - \dot{W}_{\text{out}}$, as shown in Fig. 7(a), then $\dot{W}_{\text{in,net}} = -\dot{W}_{\text{rev}}$, or

$$\dot{W}_{\text{in,net}} = \dot{Q}_{s,\text{tot}} \left(\frac{T_{\text{ref}}}{T_s} - 1 \right). \tag{5}$$

The ERE is defined as the total building energy ($\dot{W}_{\text{in}} + \dot{Q}_{s,\text{tot}}$) minus recovered energy for use elsewhere on site ($\dot{W}_{\text{out}}$), divided by the IT energy [20], or

$$\text{ERE} = \frac{\dot{W}_{\text{in,net}} + \dot{Q}_{s,\text{tot}}}{Q_{s,\text{tot}}}. \tag{6}$$

Incorporating (5) into (6) yields an expression for the minimum possible ERE when no entropy is generated throughout the cooling system

$$\text{ERE}_{\text{min}} = \frac{T_{\text{ref}}}{T_s}. \tag{7}$$

Therefore, it is clear that lower ERE values are theoretically possible with colder ambient environments since T_s is constant. Interestingly, (7) suggests that an ERE below one is possible if zero losses are seen in the system and waste energy recovery is 100% efficient. In reality, losses in the cooling system, combined with the high inefficiency of common waste energy recovery mechanisms (e.g., absorption refrigeration and the organic Rankine cycle), often raise the ERE to values above one.

Equation (7) can also be derived by considering the fact that the most efficient cooling system contains no exergy destruction. To examine this case, one must consider the equation for exergy destruction in a process [19]

$$\dot{\Psi}_d = \sum \dot{m}_i \psi_i - \sum \dot{m}_e \psi_e + \sum_j \left(1 - \frac{T_{\text{ref}}}{T_j}\right) \dot{Q}_j + \dot{W}_{\text{in,net}} \tag{8}$$

where the subscripts i and e represent inlet and exit streams, respectively, and the exergy associated with a stream is

$$\psi = \left(h - T_{\text{ref}} s + \frac{1}{2} V^2 + gz\right) - (h_{\text{ref}} - T_{\text{ref}} s_{\text{ref}} + g z_{\text{ref}}) \tag{9}$$

where h is enthalpy, s is entropy, V is speed, g is gravitational acceleration, and z is elevation. If only thermal effects are considered for an incompressible fluid, then (9) simplifies to

$$\psi = c_p (T - T_{\text{ref}}) - c_p T_{\text{ref}} \ln\left(\frac{T}{T_{\text{ref}}}\right). \tag{10}$$

If the cooling system is closed, then the control volume can be drawn such that there are no inflows and outflows for the system, and the first two terms on the right-hand side of (8) are zero. Furthermore, in the limit of zero exergy destruction through the cooling system, then $\dot{\Psi}_d = 0$, so

$$0 = \left(1 - \frac{T_{\text{ref}}}{T_s}\right) \dot{Q}_{s,\text{tot}} + \dot{W}_{\text{in,net}}. \tag{11}$$

Applying (6) on this result recovers (7). This result shows that the minimum possible ERE is achieved when the streams through the cooling system lose no exergy.

The exergy destruction can also be tied to the ERE directly using (8). For a closed cooling system, the equation simplifies to

$$\dot{\Psi}_d = \left(1 - \frac{T_{\text{ref}}}{T_s}\right) \dot{Q}_{s,\text{tot}} + \dot{W}_{\text{in,net}}. \tag{12}$$

Incorporating (6) into (12) yields

$$\text{ERE} = \frac{T_{\text{ref}}}{T_s} + \frac{\dot{\Psi}_d}{\dot{Q}_{s,tot}}. \tag{13}$$

This analysis can be summarized in the following insights.

1) The minimum ERE corresponds to zero exergy destruction, as expected.
2) The ERE depends on the ratio of destroyed work ($\dot{\Psi}_d$) to available heat ($\dot{Q}_{s,\text{tot}}$).
3) The minimum ERE is equal to the ratio T_{ref}/T_s, showing that colder climates generally favor lower ERE values, assuming a constant server temperature.

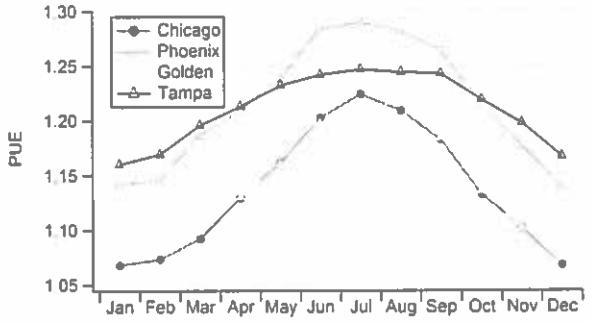

Fig. 8. Variation of PUE with location.

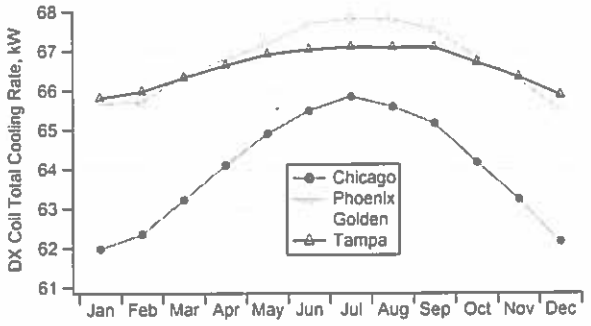

Fig. 9. Variation of cooling coil total cooling rate.

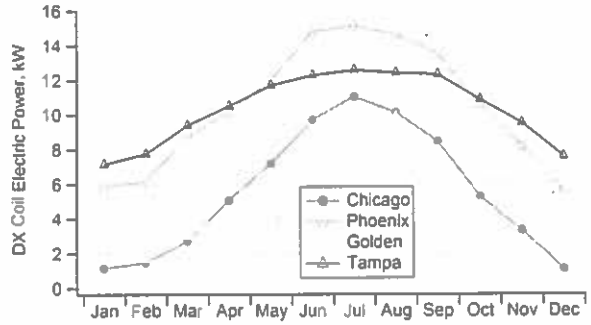

Fig. 10. Variation of cooling coil power consumption with location.

Equation (13) provides a means of calculating the overall exergy destruction for a closed cooling system based on ERE, server heat output, server temperature, and ambient temperature.

V. Results for DX Cooling

Output parameters from EP are averaged and then plotted for each month across the four locations. Figs. 8–13 compare the outdoor dry-bulb temperature, PUE values, CRAC and HVAC power consumption, DX coil power consumption and its SCOP, and exergy destruction across the four locations. The figures clearly show that additional cooling energy is needed for summer months, adversely impacting the PUE. Furthermore, less cooling energy is needed for colder climate regions (Chicago, IL, and Golden, CO) compared to warmer climate regions (Phoenix, AZ, and Tampa, FL).

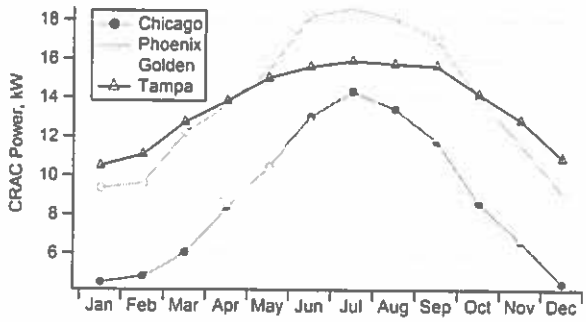

Fig. 11. CRAC total power consumption.

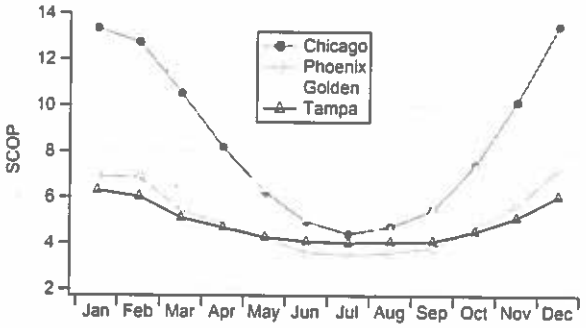

Fig. 12. CRAC SCOP variation with location.

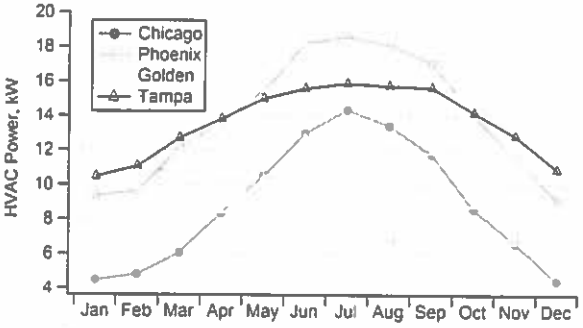

Fig. 13. Variation of HVAC total power consumption.

The exergy destruction calculation of (4) indicates that two parameters affect server exergy destruction within a data center: 1) the ambient or surrounding temperature in which the system is placed (T_{ref}), and 2) the difference in air temperature between the server inlet and exit, $\Delta T = T_{\text{out}} - T_{\text{in}}$. The ambient temperature (T_{ref}) is important in that it is related to the ERE per (13). The temperature difference (ΔT) is important in that it determines the extent to which exergy (potential) is being utilized or wasted, depending on the situation at hand. Equation (13) shows that this wasted energy directly correlates to an increase in ERE. In the case of a data center, the higher the exhaust temperature of a server, the less potential is being wasted since increasing the air temperature increases its ability to do useful work. It should be noted that increasing ΔT also reduces the airflow across the server, meaning less fan work, and therefore, less $\dot{W}_{\text{in,net}}$, and thus a lower ERE. To illustrate this concept, consider that $\dot{Q}_s = \dot{m}_s c_{p,a} \Delta T$. It can be shown

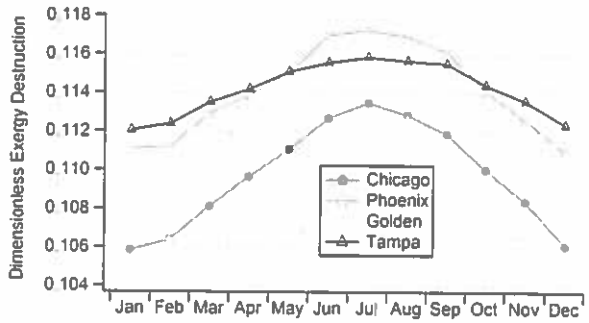

Fig. 14. Variation of dimensionless server exergy destruction with location.

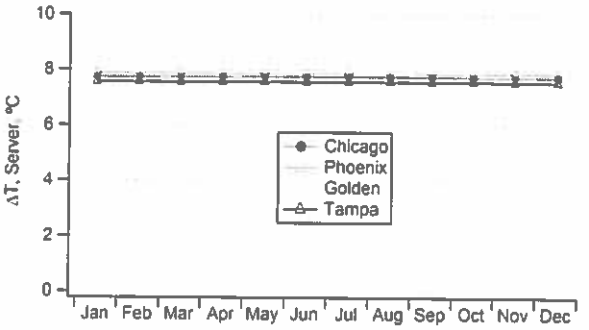

Fig. 15. Server temperature difference across the four locations for DX cooling.

using (4) that the dimensionless server exergy destruction is

$$\frac{\dot{\Psi}_{d,s}}{n_s \dot{Q}_s} = T_{\text{ref}} \left[\frac{1}{\Delta T} \ln \left(\frac{T_{\text{out}}}{T_{\text{in}}} \right) - \frac{1}{T_s} \right]. \tag{14}$$

The equation shows that $\dot{\Psi}_{d,s}$ increases with $\ln(T_{\text{out}}/T_{\text{in}})/\Delta T$, meaning that a larger ΔT indicates less exergy destruction. Furthermore, since the first term in the brackets is larger than the second, the exergy destruction increases with T_{ref}. Finally, if T_{in} increases but ΔT remains constant, then the ratio $T_{\text{out}}/T_{\text{in}}$ decreases, resulting in a decreased $\dot{\Psi}_{d,s}$.

Keeping these factors in mind, the trends shown in Fig. 14 depict that higher ambient (reference) temperatures will have higher dimensionless server exergy destruction per (14). However, when the reference temperature is held constant, the parameters that affect the exergy destruction are the server inlet and exit temperatures. A higher ΔT across the server would result in a lower value of exergy destruction, keeping all other factors constant. To illustrate this, consider the fact that the Golden, CO, has a slightly larger outdoor temperature than Chicago, IL, in February per Fig. 4. However, it has a slightly larger ΔT than Chicago, IL, per Fig. 15 (which is believed to be due to a difference in elevation since the trend is independent of month). Fig. 14 shows essentially the same exergy destruction between the two locations for February, which suggests that the Golden, CO, larger ΔT is balanced by its higher T_{ref} for that month.

Note that the calculated server temperatures, as shown in Fig. 16, are consistent with values reported in [21] where average CPU, general public utilities, and RAM temperature are reported to be 65 °C, 75 °C, and 85 °C, respectively.

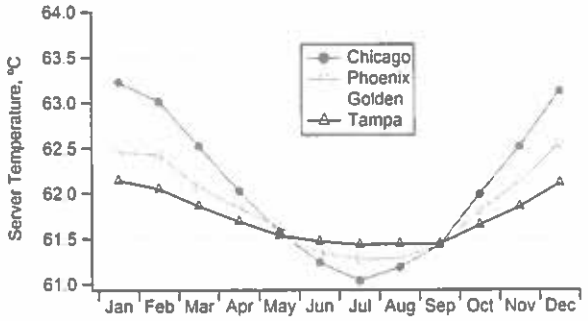

Fig. 16. Server temperature across the four locations for DX cooling.

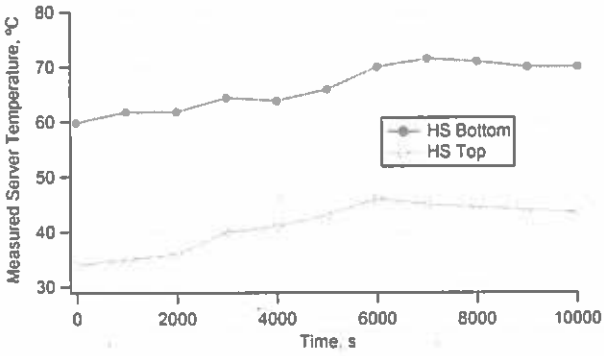

Fig. 17. Measured server temperature [17].

Furthermore, the calculated values also lie in the range of measured server temperatures given in [22]. The trend from this paper is shown in Fig. 17 for comparison.

VI. Passive Cooling Techniques

As seen in the above analysis, the base cooling option (DX Cooling) is not the most viable option for every location, particularly in hot and dry climates like those of the southwest U.S. (e.g., Phoenix, AZ) or hot and humid climates like those in the southeast (e.g., Tampa, FL). Hence, depending on the climate in which to deploy your modular data center, additional cooling techniques on top of the base case can be added to enhance performance factors such as PUE and SCOP and reduce the HVAC and hence overall facility electricity consumption.

Passive cooling techniques such as evaporative cooling (direct and indirect) as well as free air cooling can be effectively employed in modular data centers to enhance cooling efficiency and reduce power consumption.

A. Direct Evaporative Cooling

DEC is a technique to remove heat simply by evaporating water within an airstream. It differs from traditional mechanical cooling systems (such as DX CRAC units or chilled water CRAH units) in that they require practically no electricity to cool the air, making them an economical option to use in regions where the summers are dry yet water is available. Moreover, if the ambient conditions permit, the incoming outdoor air can bypass the evaporative cooler and the system can operate in economizer mode as well, thus even saving

Fig. 18. DX-DEC HVAC schematic as displayed in EP.

power required to run the pump of the evaporative cooler. Fig. 18 shows the schematic of a hybrid DX-evaporative cooler system modeled in EP.

Within EP, the Evaporative Cooler Direct Research Special Object is used to model this system. A separate availability schedule is specified to turn the evaporative cooler ON and OFF, depending on the ambient air temperature. A sensor placed on the outdoor air node senses the ambient air and is controlled by the object Outdoor Air Controller. Based on the ambient temperature, the evaporative cooler operates as per the following logic.

1) If $T_o < 12$ °C, then cutoff the outside air.
2) If 12 °C $< T_o \leq 28$ °C, then run in economizer mode and mix with return air to meet zone cooling setpoint.
3) If $T_o > 28$ °C, then run the evaporative cooler.

The evaporative cooler runs to meet the setpoint at its outlet, Node 1, which is equal to that of the supply equipment outlet node, Node 3. If this temperature at Node 1 is below the setpoint, then return air is introduced to meet the same setpoint at Node 2, the exit of the mixing box node. If the temperature at Node 1 is greater than the return air temperature, then the return air is exhausted using a relief valve located in the mixing box and the DX coil runs to meet the required setpoint. In this manner, the DX coil runs for a smaller fraction of time, thus saving a significant amount of electric power since the power consumption of the cooler pump is negligible compared to that of the DX coil's compressor. The specifications for the DX-evaporative cooling system are shown in Table V.

B. Free Air Cooling

An air-side economizer brings outside air into the data center and distributes it to the servers. The hot zone return air is fed into a mixing box where it is mixed in proportion with the cooler outside air to achieve the required zone cooling setpoint. The outdoor air controller uses the following logic to mix the outdoor and return air streams.

TABLE V
DX-EVAPORATIVE COOLING SYSTEM SPECIFICATIONS

Object	Specification
System type	Hybrid direct evaporative cooler & DX type A/C with electric heating
Thermostat type	Dual-zone thermostat
Cooling Setpoint	29.3°C
Design Supply Air Temp	14°C
Supply Fan	Single speed on/off fan
Air distribution unit	Single-duct VAV with no reheat
Cooling coil COP	4.6
Evaporative Cooler	
System efficiency	0.7
Rated Pump Power	30 W

Fig. 19. DX-free air cooling HVAC schematic as displayed in EP.

1) If T_o < 12 °C or T_o > 28 °C, then cut off the outside air.
2) Otherwise, mix with return air to meet supply outlet node setpoint.

The hybrid DX-free air cooling system has the same specifications as that of the individual DX cooling system. The DX coil is set to autosize for all three cases. The supply equipment outlet node is located after the main heating coil and is set to vary between 10 °C and 50 °C in order to meet the zone setpoint of 27 °C. The large variation in supply equipment setpoint allows EP to appropriately size the cooling coil. In case of oversizing, the cooling coil outlet temperature can fall below 2 °C and frost may occur, damaging the coil. In case of under-sizing, the zone may overheat.

All objects that require outside air such as evaporative coolers have built-in filters to filter the outside air and limit particle contamination within the conditioned space. Fig. 19 shows a DX cooling system with an outside air economizer.

The results from the DX cooling analysis suggested that Phoenix, AZ, has the highest mechanical PUE and hence the most HVAC power consumption. Thus, it is chosen as the location for implementing these two cooling techniques. A comparison of the mechanical PUE results, CRAC total power and HVAC system power are shown in Figs. 20–22.

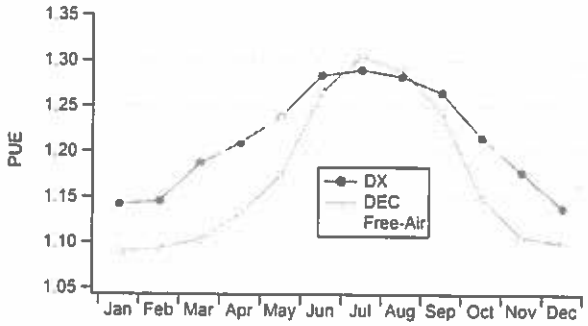

Fig. 20. Variation of PUE with cooling system for Phoenix, AZ.

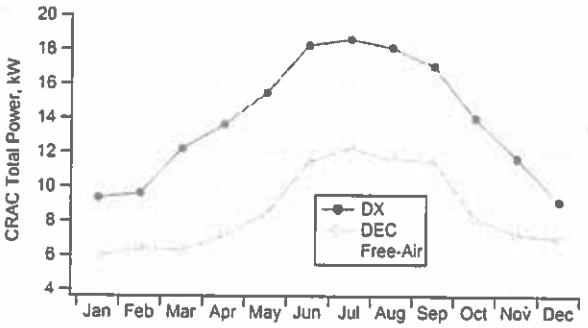

Fig. 21. Variation of CRAC total power consumption with cooling system for Phoenix, AZ.

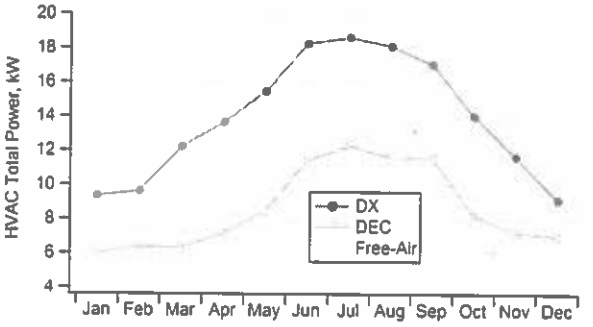

Fig. 22. Variation of HVAC total power consumption with cooling system for Phoenix, AZ.

These figures show that augmenting the base cooling system with either of these cooling techniques produces great savings in terms of HVAC power and hence elevates the mechanical cooling efficiency (mechanical PUE). Figs. 23–26 present the DX coil total cooling rate and its power consumption, the evaporator cooler pump power, its volume of water used, and lastly the exergy destruction for the facility for the three cooling systems.

The trend in evaporative cooler power also depicts the time for which it runs during the year. During the winter months of December through February, it is mostly powered OFF. However, in the summer months from May through August, it runs throughout on full power because of the hot and dry outside air, and hence maximum savings in terms of cooling power are reported during this period.

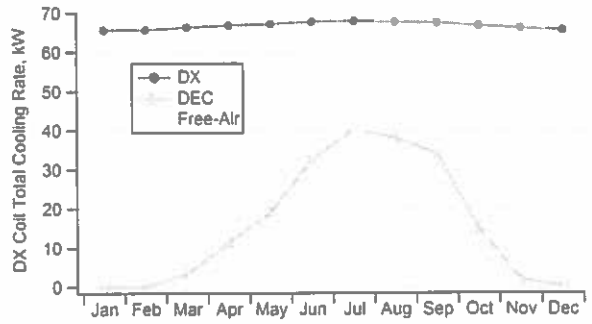

Fig. 23. Variation of cooling coil total cooling rate for Phoenix, AZ.

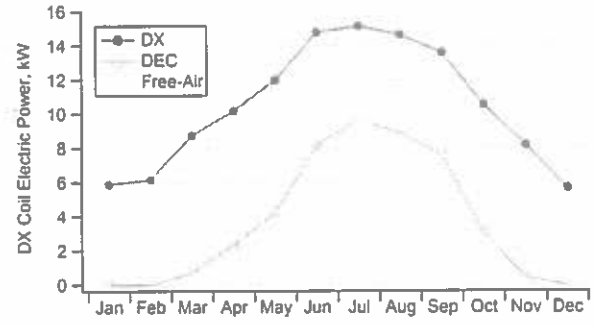

Fig. 24. Variation of cooling coil total power consumption for Phoenix, AZ.

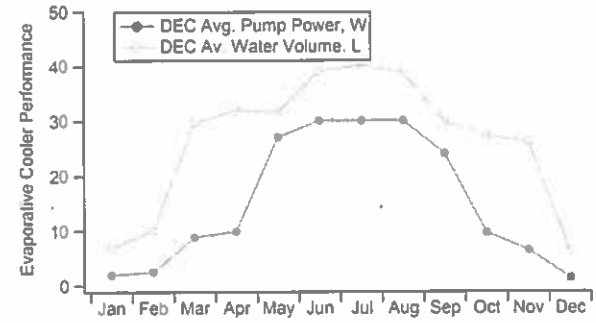

Fig. 25. Evaporative cooler pump power and water usage for Phoenix, AZ.

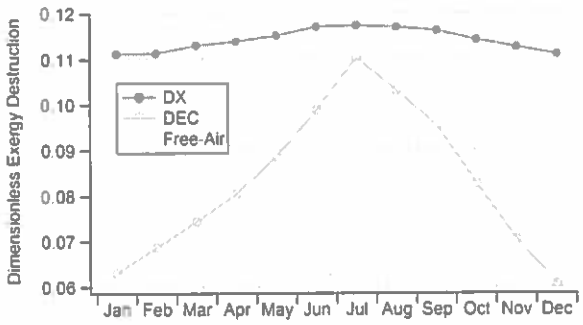

Fig. 26. Variation of dimensionless server exergy destruction with cooling system for Phoenix, AZ.

Table VI summarizes the annual average performance of the three cooling techniques for Phoenix. The dry climate points to using DEC as the best cooling technique.

TABLE VI
DX, EVAPORATIVE, AND FREE AIR COOLING PERFORMANCE SUMMARY, PHOENIX, AZ

Parameter	DX	DX + DEC	DX + Free Air
PUE	1.21	1.17	1.20
CRAC Power (kW)	13.96	8.65	8.91
HVAC Power (kW)	13.96	8.65	8.91
DX Coil Cooling Rate (kW)	66.77	16.47	28.79
DX Coil Power (kW)	10.48	3.78	5.50

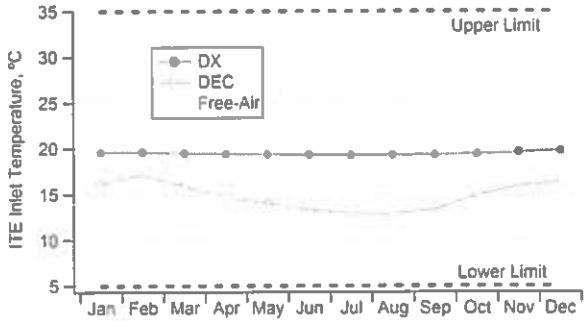

Fig. 27. IT equipment inlet temperature for the three cooling systems.

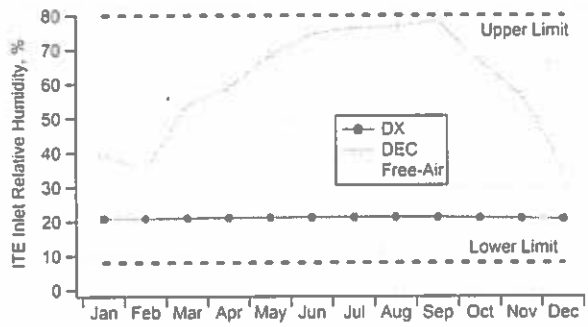

Fig. 28. IT equipment inlet relative humidity for the three cooling systems.

TABLE VII
WINTER, SUMMER, AND ANNUAL PUE VALUES FOR DX COOLING

Location	Winter PUE	Summer PUE	Annual PUE
Chicago, IL	1.08	1.20	1.14
Phoenix, AR	1.15	1.27	1.22
Golden, CO	1.10	1.20	1.14
Tampa, FL	1.17	1.24	1.21

VII. RESULTS AND DISCUSSION

The IT equipment inlet temperature profile and inlet relative humidity are compared against ASHRAE class A3 limits. The results are presented in Figs. 27 and 28. The figures indicate that the limits are obeyed for all three cooling systems throughout the year.

A summary of the mechanical PUE results for DX cooling are presented in Table VII.

TABLE VIII
MECHANICAL PUE VALUES FOR PHOENIX, AZ, USING DX, EVAPORATIVE, AND FREE AIR COOLING

Method	Winter PUE	Summer PUE	Annual PUE
DX	1.15	1.27	1.22
DX + DEC	1.09	1.26	1.17
DX + Free Air	1.13	1.29	1.21

TABLE IX
EXERGY DESTRUCTION CALCULATION DATA FOR PHOENIX, AZ, AND CHICAGO, IL

Metric	Source	Winter	Summer
PHOENIX, AZ			
PUE	Table VII	1.15	1.27
Server Temp. (°C)	Fig. 15	62.5	61.4
Ambient Temp. (°C)	Fig. 3	12.0	33.3
Server Exergy Destruction (kW)	Fig. 14	5.56	5.86
CHICAGO, IL			
PUE	Table VII	1.08	1.20
Server Temp. (°C)	Fig. 15	63.2	61.0
Ambient Temp. (°C)	Fig. 3	-5.0	24.0
Server Exergy Destruction (kW)	Fig. 14	5.29	5.68

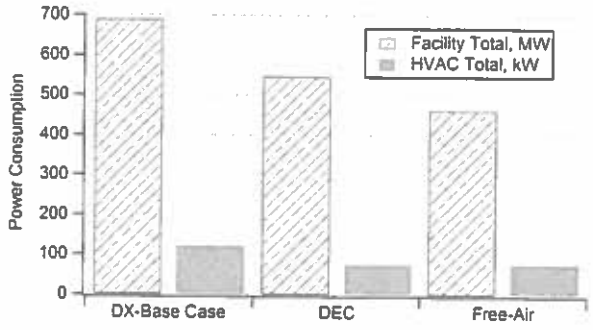

Fig. 29. Comparison of annual total facility and HVAC system power consumption for Phoenix, AZ.

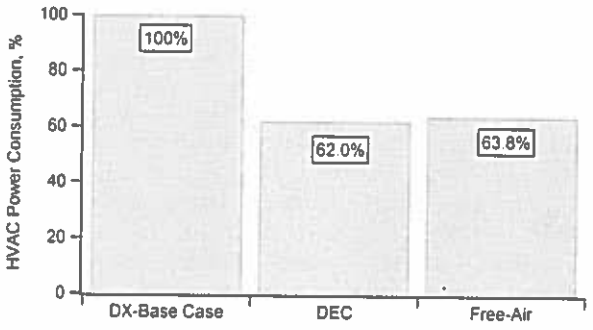

Fig. 30. Comparison of HVAC power consumption as a percentage of the base case (DX cooling), Phoenix, AZ.

The mechanical PUE values for the hybrid systems are summarized in Table VIII.

Table VII enables the calculation of the overall system exergy destruction values for DX cooling. Since there is no waste energy recovery, $\dot{W}_{out} = 0$, so ERE = PUE. The values used are summarized in Table IX for an IT load of 50 kW (Table II). The exergy destruction values are obtained by multiplying the dimensionless exergy values from Fig. 14 by the given IT load.

These results indicate that higher ambient temperatures, such as those in summers for a given location or at lower altitudes, result in larger server exergy destruction. However, other exergy destruction mechanisms like inefficiencies in the CRAC unit also play a part in overall data center exergy destruction. Modular data centers are further prone to this, due to gains through the envelope of the container, which is less significant in regular brick and mortar data centers. These factors combine to make up the vast majority of airspace exergy destruction. The remaining is contributed by auxiliary systems and equipment such as those used for backup power and networking.

In essence, for DX cooling, lowest PUE values are seen for Chicago, followed by Golden. The CRAC and HVAC power consumption are by far the lowest for Chicago. Similarly, its total cooling rate is the lowest of all, showing that it has to perform the least amount of work. Moreover, its coil power consumption (input power) and hence its SCOP are by far the lowest and highest, respectively. Hence, DX cooling is very well suited for colder locations like Chicago where the cold outside air cools the condenser (air-to-air loop) better by raising the system's efficiency.

As can be seen from Figs. 20–24, the inclusion of additional cooling systems on top of DX cooling greatly reduce the load on the DX cooling system, which helps to drastically lower its power consumption and total cooling rate. A comparison of the total facility electricity consumption and HVAC system power consumption is given in Fig. 29. The results clearly demonstrate the savings in power consumption by adapting hybrid cooling approaches consisting of passive cooling techniques on top of the base DX cooling system. The power consumption of these hybrid cooling techniques as a percentage of the DX base case is shown in Fig. 30.

Tables VII and VIII show that the greatest energy savings are seen in the case of adapting an evaporative cooling approach, followed by that of free air cooling. This is because the evaporator cooler can function in economizer mode—as well as operating independently—to meet the cooling load, thus saving excess power that is consumed by running the DX coil and hence improving the PUE. Moreover, the results show that for a hot and arid place like Phoenix, AZ, evaporative cooling can work very well in the hot and dry summer months to adequately cool the facility and reduce power consumption and electricity cost. In case of a hybrid DX-evaporative cooling system, the colder night air can be used to run the system in economizer mode and save further energy. Moreover, this combination works better for a hot

place like Phoenix, AZ, where the daytime outdoor temperatures would prohibit the use of air-side economization, and hence the sole reliance would fall on the DX system, increasing the power consumption (and hence PUE) compared to the DX-evaporative cooling case. Similarly, during the winter months, the evaporative cooler can aid the DX system during the hotter hours of the day, thus achieving slightly better PUE values than free air cooling alone.

Free air cooling is second best to evaporative cooling because of the relatively limited utilization of ambient air. Moreover, the results supplement the findings of Depoorter *et al.* [7] that PUE values for free air cooling rise in the summer months due to lesser availability of outside air, as opposed to other techniques like DEC. However, in periods of time where outside air cannot be brought in to cool the facility, the only option is to run the power-hungry DX coil.

However, the extent to which each of these cooling techniques can be utilized depends on the outdoor dry and wet-bulb temperatures. In places where they are not suitable to run for extended periods of time, such as the hot and humid conditions of Tampa, FL, the cost of installing or modifying a facility may not overcome the energy savings that are brought about by utilizing these passive cooling techniques. A case-by-case study would then be necessary, which can account for particulars (e.g., the extent of dehumidification, its associated cost and its impact on the overall energy consumption). The present paper looks at overall scenarios and compares various sites using a time-averaged analysis.

VIII. Conclusion

Energy usage modeling of various modular data center cooling systems has been undertaken using the open source software EP. Four locations across the United States have been initially modeled using DX cooling as the base system. The results suggest that in hotter climates near the southern belt, augmenting the base system with additional techniques such as direct evaporative and free air cooling can produce energy savings of 38% and 36%, respectively, and help to take the load off the DX system. The results show that DEC has the most effect on reducing energy consumption in a hot and dry climate like Phoenix since the evaporative cooler pump power is negligible compared to the DX system compressor power. Furthermore, free air cooling can be utilized when outdoor temperatures are suitable enough, either as a stand-alone cooling option or using evaporative cooler in economizer mode.

The modeling work further suggests that the COP of the DX cooling coil significantly affects its power consumption, and raising the COP from a typical value of 3.0 to 4.6 can reduce the peak summer PUE values from 1.65 down to 1.40. Furthermore, this paper gives insight into an optimum IT equipment inlet temperature of 23 °C, exceeding which will reduce the CRAC/HVAC system power but increase the server fan power, thus having a negative effect on overall energy consumption and hence PUE values. Thus, a tradeoff exists between IT equipment and HVAC power, and a balanced temperature for the facility must be maintained to achieve optimum results.

Lastly, a second-law analysis of the servers suggests that their dimensionless exergy destruction is a function of temperature only, and the biggest contributor is the ambient temperature followed by the server inlet-outlet temperature difference, ΔT. Simulation results suggest that by lowering the cooling setpoint, the server inlet temperature, and hence the resulting server surface temperature can be reduced. This is possible by suitably utilizing passive cooling techniques, which can allow the data center to operate at lower temperatures without raising power consumption and hence utility costs. Note, however, that lowering the cooling setpoint using DX only increases the compressor power, causing a rise in PUE.

IX. Future Work

This paper can be extended to other types of economization, such as water-side economization, and indirect evaporative cooling. In addition, exergy destruction calculations should be applied to economization techniques to suggest cooling solutions for different climates and their minimum possible ERE values.

Acknowledgment

Any opinions, findings, and conclusions or recommendations expressed in this material are those of the author(s) and do not necessarily reflect the views of the National Science Foundation. The authors would like to appreciate the conversations with Dr. A. Fleischer.

References

[1] S.-W. Ham, M.-H. Kim, B.-N. Choi, and J.-W. Jeong, "Energy saving potential of various air-side economizers in a modular data center," *Appl. Energy*, vol. 138, pp. 258–275, Jan. 2015.

[2] S.-W. Ham, J.-S. Park, and J.-W. Jeong, "Optimum supply air temperature ranges of various air-side economizers in a modular data center," *Appl. Thermal Eng*., vol. 77, pp. 163–179, Apr. 2015.

[3] H. Endo, H. Kodama, H. Fukuda, T. Sugimoto, and T. Horie, "Effect of climatic conditions on energy consumption in direct fresh-air container data centers," *Sustain. Comput. Inf. Syst.*, vol. 6, pp. 17–25, Apr. 2015.

[4] R. A. Steinbrecher and R. Schmidt, "Data center environments—ASHRAE's evolving thermal guidelines," *ASHRAE J*., 2011.

[5] H. Zhang, S. Shao, H. Xu, H. Zou, and C. Tian, "Free cooling of data centers: A review," *Renew. Sustain. Energy Rev.*, vol. 35, pp. 171–182, Apr. 2014.

[6] A. Qouneh, C. Li, and T. Li, "A quantitative analysis of cooling power in container-based data centers," in *Proc. IEEE Int. Symp. Workload Characterization (IISWC)*, Nov. 2011, pp. 61–71.

[7] V. Depoorter, E. Oro, and J. Salom, "The location as an energy efficiency and renewable energy supply measure for data centers in Europe," *Appl. Energy.*, vol. 140, pp. 338–349, Mar. 2015.

[8] D. Demetriou, "Effectively applying the expanded ASHRAE guidelines in your data center," IBM Systems, Somers, NY, USA, IBM White Paper XBW03029-USEN-00, Nov. 2015.

[9] H. A. Alissa *et al.*, "Chip to chiller experimental cooling failure analysis of data centers: The interaction between IT and facility," *IEEE Trans. Compon., Packag., Manuf. Technol.*, vol. 6, no. 9, pp. 1361–1378, Sep. 2016.

[10] *Huawei Modular Data Center IDS-1000A (All-In-One Container Data Center)*, accessed on Jun. 7, 2017. [Online]. Available: http://actfornet.com/huawei-it/ids1000a.html

[11] H. A. Alissa, "Innovative approaches of experimentally guided CFD modeling for data centers," in *Proc. SEMI-THERM Symp.*, Apr. 2015, pp. 176–184.

[12] M. Iyengar, R. R. Schmidt, H. Hamann, and J. VanGilder, "Comparison between numerical and experimental temperature distributions in a small data center test cell," in *Proc. ASME InterPACK Conf.*, vol. 1, 2007, pp. 819–826.

[13] M. Iyengar and R. Schmidt, "Analytical modeling for thermodynamic characterization of data center cooling systems," *J. Electron. Packag.*, vol. 131, no. 2, p. 021009-9, 2009.
[14] D. O. Energy. (2010). *EnergyPlus Engineering Reference*. [Online]. Available: https://energyplus.net/sites/default/files/pdfs_v8.3.0/EngineeringReference.pd
[15] *Google SketchUp*, accessed on Jun. 7, 2017. [Online]. Available: http://www.sketchup.com
[16] *NREL Weather Data*, accessed on Jun. 7, 2017. [Online]. Available: https://energyplus.net/weather-region/north_and_central_america_wmo_region_4/USA%20%20
[17] K. Fouladi, A. P. Wemhoff, L. Silva-Llanca, K. Abbasi, and A. Ortega, "Optimization of data center cooling efficiency using reduced order flow modeling within a flow network modeling approach," in *Proc. ASME*, 2014, pp. 1–11.
[18] A. Bhalearo, K. Fouladi, L. Silva-Llanca, and A. P. Wemhoff, "Rapid prediction of exergy destruction in data centers due to airflow mixing," *Numer. Heat Transf., A. Appl.*, vol. 70, no. 1, pp. 48–63, 2016.
[19] R. E. Sonntag, C. Borgnakke, and G. J. Van Wylen, *Exergy Fundamentals Thermodynamics*, 5th ed. New York, NY, USA: Wiley, 1998, pp. 393–406.
[20] M. Patterson *et al.*, "ERE: A metric for measuring the benefit of reuse energy from a data center," The Green Grid, Beaverton, OR, USA, White Paper 29, 2010.
[21] O. Van Geet, "Trends in data center design-ASHRAE leads the way to large energy savings," in *Proc. ASHRAE Conf.*, Denver, CO, USA, 2014.
[22] M. Ibrahim *et al.*, "Characterization of a server thermal mass using experimental measurements," in *Proc. InterPACK MEMS NEMS*, vol. 2, 2011, pp. 577–583.
[23] R. Khalid, Y. Joshi, and A. P. Wemhoff, "Rapid modeling tools for energy analysis of modular data centers," in *Proc. IEEE ITHERM*, Sep. 2016, pp. 1444–1452.

Rehan Khalid received the B.S. degree in mechanical engineering from the Ghulam Ishaq Khan Institute of Engineering Sciences and Technology, Topi, Pakistan, in 2012, and the M.S. degree in mechanical engineering from the Georgia Institute of Technology, Atlanta, GA, USA, in 2014. He is currently pursuing the Ph.D. degree in mechanical engineering with Villanova University, Villanova, PA, USA.

From 2012 to 2014, he was a Trainee Engineer with various national and multinational consulting firms on projects related to the energy sector.

Mr. Khalid was a recipient of the Fulbright Fellowship from the U.S. Department of State for pursuing his master's degree.

Aaron P. Wemhoff received the B.S. degree in mechanical engineering from the University of Virginia, Charlottesville, VA, USA, in 2000, and the M.S. and Ph.D. degrees in mechanical engineering from the University of California, Berkeley, CA, USA, in 2002 and 2004, respectively.

From 2005 to 2008, he was a Staff Engineer with the Lawrence Livermore National Laboratory, Livermore, CA, USA. Since 2008, he has been a Faculty Member with the Mechanical Engineering Department, Villanova University, Villanova, PA, USA. He has authored more than 50 articles. His current research interests include energy-efficient design of buildings and data centers as well as molecular modeling of nanoscale systems, theoretical development of thermodynamic, and thermal transport theories.

Dr. Wemhoff is currently the Chair of ASME K-20 Committee on Computational Heat Transfer.

Yogendra Joshi (SM'03–F'12) received the Ph.D. degree in mechanical engineering and applied mechanics from the University of Pennsylvania, Philadelphia, PA, USA, in 1984.

He is a Professor and John M. McKenney and Warren D. Shiver Distinguished Chair with the G.W. Woodruff School of Mechanical Engineering, Georgia Institute of Technology, Atlanta, GA, USA, where he is the Principal Investigator of the Office of Naval Research Consortium for Resource-Secure Outposts and the Site Director of the National Science Foundation Industry/University Cooperative Research Center on Energy Efficient Electronic Systems. His current research interests include multiscale thermal management.

Dr. Joshi is an elected Fellow of ASME and the American Association for the Advancement of Science. He was a co-recipient of the ASME Curriculum Innovation Award in 1999, the Inventor Recognition Award from the Semiconductor Research Corporation in 2001, the ASME Electronic and Photonic Packaging Division Outstanding Contribution Award in Thermal Management in 2006, the *ASME Journal of Electronics Packaging* Best Paper of the Year Award in 2008, the IBM Faculty Award in 2008, the IEEE SemiTherm Significant Contributor Award in 2009, the IIT Kanpur Distinguished Alumnus Award in 2011, the ASME InterPack Achievement Award in 2011, the ITherm Achievement Award in 2012, and the ASME Heat Transfer Memorial Award in 2013.